

Analysis of FBG Reflection Spectra Under Anti-symmetrical Strain Distributions Using the Approximated Transfer Matrix Model

Aydin Rajabzadeh^{a,b}, Richard C. Hendriks^a, Richard Heusdens^a, and Roger M. Groves^b

^a Circuits and Systems group, Delft University of Technology, Delft, 2628 CD, The Netherlands

^b Structural Integrity and Composites group, Faculty of Aerospace Engineering, Delft University of Technology, Delft, 2629 HS, The Netherlands

ABSTRACT

In this paper, we used the efficient formulation of the approximated transfer matrix model (ATMM) for the analysis of fibre Bragg grating (FBG) sensors' response under anti-symmetrical strain fields. Exploiting the flexible representation of the transfer matrices in this new model, we will analytically prove that any sort of anti-symmetrical strain distribution over the length of a uniform FBG sensor will result in symmetrical reflected spectra. This phenomenon had been already observed in the literature, but proving it using the classical transfer matrix model was laborious and impractical. The same discussion will be extended to the grating distribution of the FBG sensors as well. A special case of an anti-symmetrical grating distribution could be the linearly chirped FBG sensor (LCFBG), in which the grating distribution is linearly increasing over the length of the FBG. Using computer simulations, it can be seen that such a grating distribution will result in perfectly symmetrical reflected spectra. Therefore, we expect that a well-produced LCFBG, should also have a close to symmetrical reflected spectra, and deviation from this symmetry could possibly indicate undesirable birefringence effects.

Keywords: Approximated transfer matrix, fibre Bragg gratings, linearly chirped FBG, reflected spectra, strain, transfer matrix model

1. INTRODUCTION

Fibre Bragg grating (FBG) sensors have become an indispensable component of strain sensing applications, especially in the last few decades. Due to their high resistance to environmental factors, and their miniature size, they are widely used in industries such as aviation, oil and gas, and civil engineering.¹⁻³ Apart from the interesting mechanical properties of FBGs, another feature that makes them attractive for strain (or temperature) sensing applications is considered to be the linear relationship between the strain and the shift of the Bragg (peak) wavelength of uniform FBG sensors.^{1,4} Under uniform strain fields, the reflected spectrum of the FBG sensor will keep its symmetry, and the aforementioned linear relationship holds. In addition, using coupled mode theory, the FBG reflected spectra can be characterised by a closed form function of wavelength and the characteristic physical parameters of the sensor.⁵ However, when the sensor is subject to non-uniform strain fields, the reflected spectra becomes more complicated with several local peaks. In such non-uniform strain fields, using the linear relationship between the mean strain and the shift of the Bragg wavelength will in general result in an error of up to tens of micro-strains. In such strain fields, using the coupled mode theory to derive an analytical expression for the reflected spectra will become cumbersome and impractical. In order to solve this problem one of the most commonly used methods for analysis of FBG reflected (and transmitted) spectra under arbitrary axial strains (or grating structure) is the transfer matrix model.⁶ The basic assumption in this model is to consider a piece-wise uniform strain field (or grating structure) for the sensor. In other words, the length of the sensor is assumed to be divided into smaller segments, all of which are undergoing a uniform strain. In 1987, Yamada and Sakuda formulated the transfer matrices that characterise the interaction between the electric waves of consecutive segments in this model, and ultimately, described the overall reflected spectra by multiplication of all transfer matrices.⁶

Although the transfer matrix method made it possible to analyse the behaviour of FBG sensors under non-uniform strain fields, it was still difficult to extract more information about the strain field to which the sensor is subjected. In our recent work, we presented another variation of this model where we approximated the transfer matrices into a more

Further author information:

E-mail: {a.rajabzadehdizaji, r.c.hendriks, r.heusdens, r.m.groves}@tudelft.nl

compact and flexible form.⁷ This new approximated transfer matrix model (ATMM) will be the basis of the analysis in this paper, where it will be utilised to investigate the behaviour of FBG sensors under anti-symmetrical strain (grating) distributions. An example of such an anti-symmetrical grating distribution is found in the linearly chirped fibre Bragg gratings (LCFBG). Based on the discussions of this paper, it will be shown that the reflection spectra of LCFBGs are theoretically symmetrical. The paper is organised as follows. In Section 2 we present the approximated transfer matrix model and we define the parameters and assumptions used in this study. In Section 3 we will analyse the behaviour of FBG reflected spectra under anti-symmetrical strain fields, along with some discussions on the results, and Section 4 discusses the case of linearly chirped Bragg gratings. Finally, 5 concludes the paper.

2. APPROXIMATED TRANSFER MATRIX MODEL

The approximated transfer matrix model (ATMM) is derived from the transfer matrix model (TMM).⁶ As such, the underlying assumptions for the ATMM are similar as for the TMM. Among these is the assumption that the FBG sensor of length L is divided into M equal segments of length Δz (with $L = M\Delta z$). The forward propagating electric wave inside the core of the FBG sensor entering the i 'th segment will be called A_i and the backward propagating electric wave reflected from the i 'th segment will be called B_i . A schematic view of this structure is shown in Fig. 1.

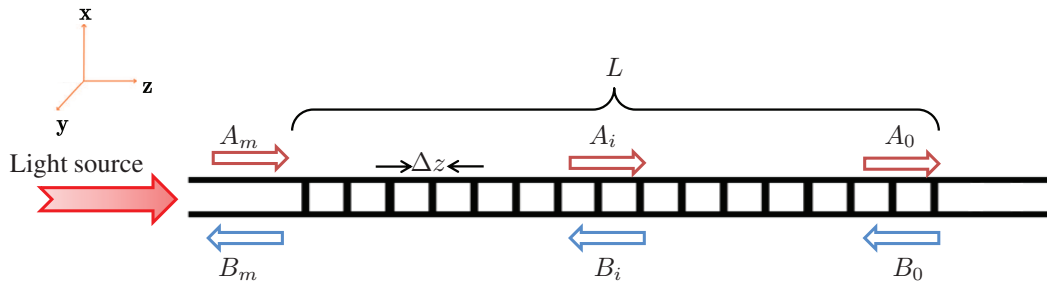


Figure 1: Schematic view of the FBG structure.

We showed that for a sufficiently small Δz , the relationship between the forward and backward electric waves is characterized as⁷

$$\begin{pmatrix} A_i \\ B_i \end{pmatrix} = F_i \begin{pmatrix} A_{i-1} \\ B_{i-1} \end{pmatrix}, \quad \text{with} \quad F_i = \begin{pmatrix} e^{-j(\alpha - \alpha_i)} & -j\kappa_i \Delta z \operatorname{sinc}(\alpha - \alpha_i) \\ j\kappa_i \Delta z \operatorname{sinc}(\alpha - \alpha_i) & e^{j(\alpha - \alpha_i)} \end{pmatrix}, \quad (1)$$

in which F_i is the approximated transfer matrix of segment i , with elements F_{i11} , F_{i12} , F_{i21} and F_{i22} , and κ_i is the coupling coefficient of the i 'th segment. Note that $F_{i11} = F_{i22}^*$ and $F_{i12} = F_{i21}^*$, where $(\cdot)^*$ is the complex conjugate operator. The α and α_i parameters in (1) are defined as

$$\alpha = \frac{2\pi n_{\text{eff}} \Delta z}{\lambda} \quad \text{and} \quad \alpha_i = \frac{2\pi n_{\text{eff}} \Delta z}{\lambda_i}, \quad (2)$$

with λ being the wavelength region under investigation, λ_i being the local Bragg wavelength related to the i 'th segment, and n_{eff} being the effective refractive index of the core. Multiplying all the transfer matrices gives the relation between the electric waves of the first and the last segment, given by

$$\begin{pmatrix} A_M \\ B_M \end{pmatrix} = F \begin{pmatrix} A_0 \\ B_0 \end{pmatrix}, \quad \text{in which} \quad F = \prod_{i=1}^M F_i. \quad (3)$$

Taking into account that at the last segment there is full transmission of the incident light ($A_0 = 1$) and also no reflection of the light from the rest of the length of the optical fibre ($B_0 = 0$), the overall reflected spectra, $R(\lambda)$, can be calculated as

$$R(\lambda) = \left| \frac{B_M}{A_M} \right|^2 = \left| \frac{F_{21}}{F_{11}} \right|^2. \quad (4)$$

The main advantage of the approximated transfer matrices is its simpler representation form. The simplicity of this model does not sacrifice the accuracy significantly,⁷ but facilitates the analysis of FBG reflection spectra. In particular, the simpler form of the overall product of the approximated transfer matrices can be exploited to extract more information about the strain field to which the FBG sensor is subjected.

3. FBG SENSORS UNDER ANTI-SYMMETRICAL STRAIN DISTRIBUTIONS

In this section, we will show that an anti-symmetrical strain distribution along the length of the FBG sensor will result in a symmetrical FBG reflection spectra. This property has been observed in several papers,^{1,4} especially in studies concerning linearly chirped FBG sensors (LCFBG).^{8,9} However, proving this property using the classic TMM, for the general case of anti-symmetrical strain distributions is incredibly cumbersome, and to our knowledge no studies have investigated it so far. On the other hand, owing to its simple representation, the ATMM provides a simple proof for this property. As an example, Fig. 2a shows an arbitrarily generated anti-symmetrical strain distribution over the length of an FBG sensor with a length of 10 mm in a 500 segment model, and the resulting symmetrical reflected spectra (Fig. 2b). For this sensor, the nominal Bragg wavelength was assumed to be 1550 nm, and the refractive index modulation $dn = 2.2 \times 10^{-5}$.

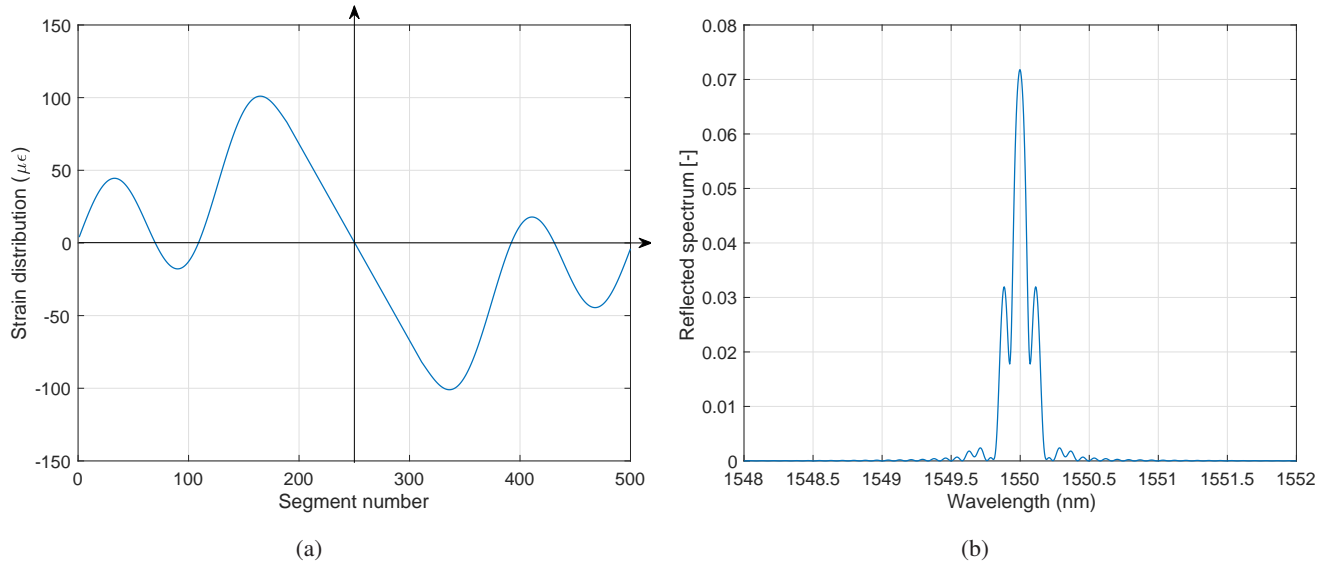


Figure 2: (a) An anti-symmetrical strain distribution, and (b) the resulting simulated FBG reflected spectra.

We assume that the variation of the coupling coefficient along the length of the sensor is negligible (i.e. $\forall i, \kappa_i \approx \kappa$). Without loss of generality, we assume that all the wavelengths are shifted so that the central wavelength of analysis is at zero. Although the reflected spectra $R(\lambda)$ as well as the approximated transfer matrices F_i are a function of the wavelength λ , we can use the transformation in (2) to the α -domain, which will facilitate the analysis. The symmetry of the reflected spectra can then be shown by proving that the reflected spectrum is an even function in the shifted α domain, i.e., $R(-\alpha) = R(\alpha)$. This implies that for the F matrix in (3) the following should hold

$$\left| \frac{F_{11}(-\alpha)}{F_{21}(-\alpha)} \right| = \left| \frac{F_{11}(\alpha)}{F_{21}(\alpha)} \right| \quad (5)$$

To prove (5) we will show that under anti-symmetrical strain distributions, the F matrix in (3) will have the following properties,

$$\begin{aligned} F_{11}(-\alpha) &= F_{11}^*(\alpha) \\ F_{21}(-\alpha) &= F_{21}(\alpha). \end{aligned} \quad (6)$$

Based on (4) it can be seen that if the conditions in (6) hold, we will have $R(-\alpha) = R(\alpha)$, i.e., a symmetrical reflection spectrum. Matrix F consists of the product of the $F_i \forall i$ matrices, associated with each segment of the FBG model. Assuming for simplicity of notation that there are an even number of segments in the model, we index the segments by index n , with $n \in \{-M/2, \dots, +M/2\}$. Let us assume that we calculate the overall F matrix in $M/2$ steps, where each step t results in an intermediate matrix F^t where the local transfer matrices of the two neighbouring segments $n = -t$ and $n = t$ are multiplied to the left and right, respectively, of the already calculated F^{t-1} matrix that originates from step $t-1$. In step $t = 0$ we have $F^t = I_2$, where I_2 is the 2-by-2-dimensional identity matrix. As an example, in step $t = 1$ we get $F^1 = F_{-1}F_1$ and in step $t = 2$ we get $F^2 = F_{-2}F^1F_2$, etc. Fig. 3 shows a schematic view of such structure.

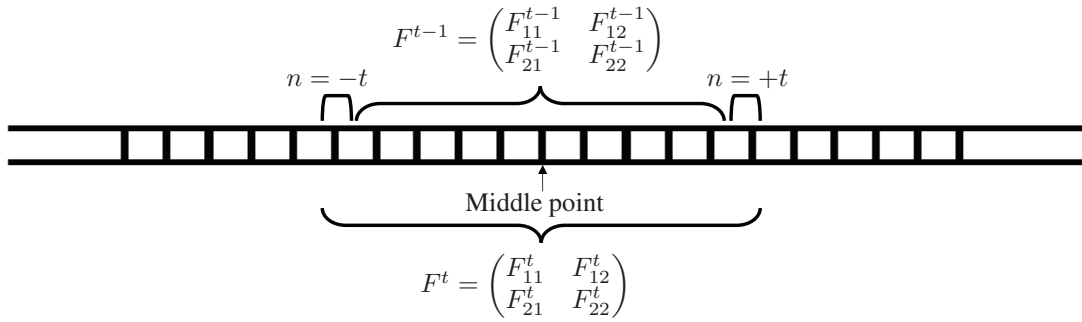


Figure 3: FBG structure in an anti-symmetrical strain distribution. The new added pair of segments with opposite strains at the two sides will preserve the properties given in (6).

As stated earlier, without loss of generality it is assumed that the local Bragg wavelength of the middle segment is at zero. Therefore, at each step of multiplication the two newly added segments involved in the multiplication will have local Bragg wavelengths with opposite signs. Suppose that at step t in the multiplication process, the following product needs to be calculated:

$$F^t = \begin{pmatrix} e^{-j(\alpha-\alpha_t)} & -jK \operatorname{sinc}(\alpha - \alpha_t) \\ jK \operatorname{sinc}(\alpha - \alpha_t) & e^{j(\alpha-\alpha_t)} \end{pmatrix} \cdot \begin{pmatrix} F_{11}^{t-1} & F_{12}^{t-1} \\ (F_{12}^{t-1})^* & (F_{11}^{t-1})^* \end{pmatrix} \cdot \begin{pmatrix} e^{-j(\alpha+\alpha_t)} & -jK \operatorname{sinc}(\alpha + \alpha_t) \\ jK \operatorname{sinc}(\alpha + \alpha_t) & e^{j(\alpha+\alpha_t)} \end{pmatrix}, \quad (7)$$

with the centre matrix F^{t-1} resulting from the previous step t , and $K = \kappa\Delta z$. Also note the opposite signs of the local α_t values in the first and the third matrices in (7). Mathematical induction shows that assuming the F^{t-1} matrix has the properties of (6), adding new pairs of segments will preserve these properties. Calculating the product in (7), the elements of the F^t matrix are as follows

$$\begin{aligned} F_{11}^t(\alpha) &= e^{-j2\alpha} F_{11}^{t-1} - jK \operatorname{sinc}(\alpha - \alpha_t) e^{-j(\alpha+\alpha_t)} (F_{12}^{t-1})^* + jK \operatorname{sinc}(\alpha + \alpha_t) e^{-j(\alpha-\alpha_t)} F_{12}^{t-1} \\ &\quad + K^2 \operatorname{sinc}(\alpha + \alpha_t) \operatorname{sinc}(\alpha - \alpha_t) (F_{11}^{t-1})^*, \end{aligned} \quad (8)$$

$$\begin{aligned} F_{21}^t(\alpha) &= jK \operatorname{sinc}(\alpha - \alpha_t) e^{-j(\alpha+\alpha_t)} F_{11}^{t-1} + e^{-j2\alpha_t} (F_{12}^{t-1})^* - K^2 \operatorname{sinc}(\alpha + \alpha_t) \operatorname{sinc}(\alpha - \alpha_t) F_{12}^{t-1} \\ &\quad + jK \operatorname{sinc}(\alpha + \alpha_t) e^{j(\alpha-\alpha_t)} (F_{11}^{t-1})^*. \end{aligned} \quad (9)$$

In order to prove the validity of (8) and (9) for all t , we start by setting $t = 1$ and multiplying the first pair of segments in the middle of the FBG structure, and first prove that F^1 satisfies the properties in (6). Notice that for this case, the F^0 matrix in (8) and (9) is set to the identity matrix, which results in

$$F_{11}^1(\alpha) = e^{-j2\alpha} + K^2 \text{sinc}(\alpha + \alpha_1) \text{sinc}(\alpha - \alpha_1) = (F_{11}^1(-\alpha))^*, \quad (10)$$

$$F_{21}^1(\alpha) = jK \text{sinc}(\alpha - \alpha_1) e^{-j(\alpha + \alpha_1)} + jK \text{sinc}(\alpha + \alpha_1) e^{j(\alpha - \alpha_1)} = F_{21}^1(-\alpha). \quad (11)$$

Therefore, F^1 satisfies the conditions in (6). Now assuming that the conditions in (6) hold for step $t-1$, by plugging $-\alpha$ in (8) and (9) we get

$$F_{11}^t(-\alpha) = e^{j2\alpha} (F_{11}^{t-1}(\alpha))^* - jK \text{sinc}(\alpha + \alpha_t) e^{j(\alpha - \alpha_t)} (F_{12}^{t-1}(\alpha))^* + jK \text{sinc}(\alpha - \alpha_t) e^{j(\alpha + \alpha_t)} F_{12}^{t-1}(\alpha) + K^2 \text{sinc}(\alpha - \alpha_t) \text{sinc}(\alpha + \alpha_t) F_{11}^{t-1}(\alpha) = (F_{11}^t(\alpha))^*, \quad (12)$$

$$F_{21}^t(-\alpha) = jK \text{sinc}(\alpha + \alpha_t) e^{j(\alpha - \alpha_t)} (F_{11}^{t-1}(\alpha))^* + e^{-j2\alpha_t} (F_{12}^{t-1}(\alpha))^* - K^2 \text{sinc}(\alpha - \alpha_t) \text{sinc}(\alpha + \alpha_t) F_{12}^{t-1}(\alpha) + jK \text{sinc}(\alpha - \alpha_t) e^{-j(\alpha + \alpha_t)} F_{11}^{t-1}(\alpha) = F_{21}^t(\alpha). \quad (13)$$

It can be seen that the conditions of (6) hold for F^t . Therefore, using induction, it is proven that these properties will hold for the final product of the F_i matrices from all segments.

4. LINEARLY CHIRPED FIBRE BRAGG GRATINGS

One immediate result of this behaviour of FBG sensors is in the quality assessment of linearly chirped fibre Bragg gratings (LCFBG). The use of this type of grating is in dispersion compensation and also in several sensory applications, and as the name suggests, the grating period in these structures linearly increases along their length, which can be considered as a special case of an anti-symmetrical grating distribution. Therefore, the reflection spectra of LCFBGs should theoretically be as symmetrical as possible. As an example, Fig. 4 shows the reflection spectra of a simulated ideal LCFBG.

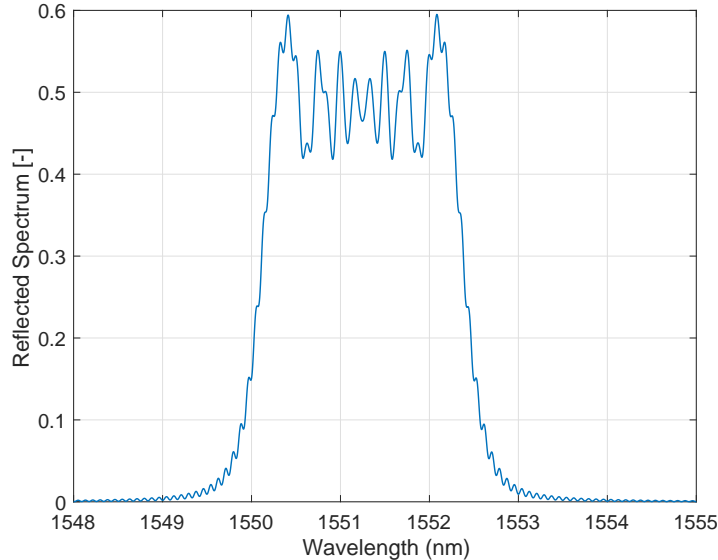


Figure 4: The symmetrical reflection spectrum of an LCFBG with $\lambda_B = 1550$ nm, $\frac{d\lambda_B}{dz} = 2.5$ nm/cm, $\delta n = 2.2 \times 10^{-4}$ and $L = 10$ mm.

This behaviour has been observed in several studies in the literature,^{1,4,8,9} and as shown in this paper, can be proven analytically using the ATMM. We conclude that a well produced LCFBG sensor should have a close to symmetrical reflected spectra, while a poorly manufactured LCFBG with undesirable birefringence effects is expected to show haphazard peaks and asymmetrical reflected spectra. An example of such a well produced LCFBG with low birefringence was presented by Li and Yao.¹⁰ In this work, they developed a method for producing LCFBGs with optical pumping in Er/Yb co-doped fibres, whose reflection spectra were much more symmetrical than LCFBGs without optical pumping.¹⁰

5. CONCLUSIONS

In this paper, we re-presented the new approximated transfer matrix model (ATMM), and exploited the compact form of the new formulation to show some interesting properties in FBG sensors. We proved that an anti-symmetrical strain distribution will result in a symmetrical reflected spectrum. This behaviour had been observed in several papers in the literature, but proving it using the transfer matrix model was laborious. The compact representation of the elements of the approximated transfer matrices made it possible to readily prove this property. This property in particular shows a good potential in quality assessment of linearly chirped FBG (LCFBG) sensors, whose grating distribution is a special case of such anti-symmetrical structures. We argued that theoretically, a perfectly produced LCFBG with low birefringence would have symmetrical reflected spectra, and deviation from symmetry could possibly indicate a poor production process with high undesirable birefringence effects.

REFERENCES

- [1] A. D. Kersey, M. A. Davis, H. J. Patrick, M. LeBlanc, K. P. Koo, C. G. Askins, M. A. Putnam, and E. J. Friebele, "Fiber grating sensors," *Journal of Lightwave Technology*, **15**, 1442-1463 (1997).
- [2] H. N. Li, D. S. Li, and G. B. Song, "Recent applications of fiber optic sensors to health monitoring in civil engineering," *Engineering Structures*, **26**, 1647-1657 (2004).
- [3] Y. Okabe, S. Yashiro, T. Kosaka, and N. Takeda, "Detection of transverse cracks in CFRP composites using embedded fiber Bragg grating sensors," *Smart Materials and Structures*, **9(6)**, 832 (2000).
- [4] K. Hill, G. Meltz, "Fiber Bragg grating technology fundamentals and overview," *Journal of Lightwave Technology*, **15**, 1263-1276 (1997).
- [5] A. Yariv, "Coupled-mode theory for guided-wave optics," *IEEE Journal of Quantum Electronics*, **9(9)**, 919-933 (1973).
- [6] M. Yamada, and K. Sakuda, "Analysis of almost-periodic distributed feedback slab waveguides via a fundamental matrix approach," *Applied Optics*, **26(16)**, 3474-3478 (1987).
- [7] A. Rajabzadeh, R. Heusdens, R. C. Hendriks, and R. M. Groves, "Calculation of the mean strain of non-uniform strain fields using conventional FBG sensors," arXiv:1803.08139 (2018).
- [8] F. Ouellette, "Dispersion cancellation using linearly chirped Bragg grating filters in optical waveguides," *Optics Letters*, **12(10)**, 847-849 (1987).
- [9] T. Erdogan, "Fiber grating spectra," *Journal of Lightwave Technology*, **15(8)**, 1277-1294 (1997).
- [10] M. Li and J. Yao, "Photonic generation of continuously tunable chirped microwave waveforms based on a temporal interferometer incorporating an optically pumped linearly chirped fiber Bragg grating," *IEEE Transactions on Microwave Theory and Techniques*, **59(12)**, 3531-3537 (2011).